Single-crystalline model spin valves using single-crystalline NiO(111) substrates

C. Mocuta,* A. Barbier,† S. Lafaye, P. Bayle-Guillemaud, and M. Panabière
CEA-Grenoble, Département de Recherche Fondamentale sur la Matière Condensée, 17, rue des Martyrs, 38054 Grenoble, France
(Received 6 February 2003; published 14 July 2003)

The preparation of fully epitaxial spin valves elaborated on NiO(111) single crystals, with permalloy ($Ni_{80}Fe_{20}$), Co, $Co_{30}Fe_{70}$, and $Co/Co_{30}Fe_{70}$ as pinned layers, is reported. The best results were obtained with permalloy being the pinned layer. A giant magneto-resistance (GMR) of 3.5% at room temperature was obtained easily. The detrimental effect of an inter-diffusion at the ferromagnet/NiO interface is shown. The role of the initial surface preparation in terms of roughness and the magnetic properties of the pinned layer are discussed. It appeared that a 0.8-nm-thick CoFe layer is an excellent and efficient wetting layer for Co. These model structures allowed a decoupled investigation of the different parameters although the nearly isotropic GMR response of these structures makes them also interesting devices. The microstructure and the exchange coupling were investigated together. At room temperature, the major effect of the exchange coupling on single crystalline NiO(111) substrates is an inversely proportional behavior of the coercive field of the pinned layer with respect to the ferromagnetic layer thickness. The effect is discussed with respect to recent models and understood as resulting from the energy losses in the antiferromagnet because of irreversible losses in the antiferromagnetic order.

DOI: 10.1103/PhysRevB.68.014416 PACS number(s): 75.47.De, 75.60.Ej

I. INTRODUCTION

The steadily increasing demand on digital storage capacity motivates a great interest in new generations of sensor devices allowing increasing the information density. The spin-valve geometry stands as the current commercial replacement for inductive hard-drive read heads.[1–3] Many studies were performed on various ferromagnetic on antiferromagnetic (FM/AF) systems and different layer combinations were tested (an overview can be found in Ref. 1). One of the most promising candidates to play the role of the AF pinning layer in spin valves is NiO with the (111) spin-uncompensated polar surface.[4,5] Read heads based on NiO have proven to possess adequate properties during read cycles on magnetic media,[1–3] because NiO is a highly corrosion resistant insulating antiferromagnet and it has a relatively high Néel temperature (520 K). NiO based sensors may thus be used in hard drive read heads, permanent magnetic memories, as well as in harsh environment applications. Moreover the use of magnetic oxide layers in spin valves to enhance the specular reflectivity[6–8] have proven to possess attractive practical properties.[9]

However, the magnetic exchange-coupling phenomenon making these devices working is still not fully understood and several models were proposed. The successful existing devices were mostly optimized within an experimental trial/error method, and no model structure was available up to now. This may be of particular importance since the interface regions are usually suspected to play the dominant role. The important contribution of the microstructure to the exchange coupling mechanisms was only recognized recently and has already motivated a number of studies involving single crystalline AF substrates which includes, e.g., CoO(111),[10] NiO(100),[11–13] and FeF_2.[14]

In the present paper we report on the elaboration of model spin-valves for which the crystalline structure is completely known. Interestingly, the enhanced exchange coupling due to the single crystal substrate, exhibiting (comparatively to sputtered structures) very large grain sizes, allows building the whole structure with permalloy ($Py=Ni_{81}Fe_{19}$). The effect of using other FM layers (Co or $Co_{30}Fe_{70}$) was also investigated, although the results are less promising. First, we recall the experimental details before showing the results, which will be discussed in the last part of the paper.

II. EXPERIMENT

The NiO(111) substrates were $5\times5\times0.5$ mm^3 platelets for the growth of spin valves and 12-mm-diameter wafers (1 mm thick) for the grazing incidence x-ray diffraction (GIXD) studies. The samples were provided, oriented to $\pm0.1°$, cut and polished by Crystal GmBH (Berlin, Germany). Prior to cutting, the NiO boule was annealed in air at 1850 K for 24 h in order to recrystallize the bulk structure. After polishing, the samples were annealed again in air at 1300 K for 3 h to heal the polishing-induced texture in the surface region. The surface was next *in situ* cleaned by a final annealing at 1000 K in O_2 (10^{-5} mbar) to remove the residual carbon contamination. X-ray measurements were then performed in ultra-high vacuum (UHV;base pressure 10^{-10} mbar). The cleanliness of the surfaces was checked by Auger electron spectroscopy. Except a tiny Ca signal corresponding to submonolayer quantities no other contamination could be identified after preparation. It was found that the Ca contamination does not affect at all the $p(2\times2)$ reconstruction of the surface.[15,16] This procedure yields flat and shiny surfaces with mosaic spreads of 0.02°–0.1°. We have shown that polar NiO(111) single crystals substrates can be prepared and exhibit a surface $p(2\times2)$ reconstruction[15–17] that heals the diverging Coulomb potential problem.[18]

The alloys films (Py, $Co_{30}Fe_{70}$) were prepared by co-evaporation using electron-bombarded rods (Co, Ni, and Fe, 99.99% purity) for which the fluxes were adjusted to obtain the right composition on the sample. The typical deposition rate was 1 Å of alloy per minute and was calibrated using a

quartz micro-balance. The Cu spacer and Au capping layers in the spin-valve sandwich were deposited using effusion cells, at 1 Å per minute deposition rate. All depositions were performed in UHV conditions. For the pinned ferromagnetic layers the growth temperature was varied from study to study. The depositions of the Cu spacer, the free ferromagnetic layer, and the Au capping layer were always performed at room temperature (RT).

The investigation of the growth mode was performed by GIXD which is particularly well suited for investigating insulating systems since it is insensitive to charge build-up. Moreover, the probed depth can easily be tuned through the incidence angle. The GIXD experiments were carried out at the ESRF (European Synchrotron Radiation Facility — Grenoble, France) (Ref. 19) on the BM32 beamline. Measurements were performed on the single-crystal surface at 18-keV photon energy (high enough to avoid fluorescence and to have access to large transfer momentum values in the reciprocal space) and at an incidence angle equal to the critical angle (0.17°) for total external reflection of the x rays at that energy, to reduce the scattering from the bulk. Following convention, the crystallographic basis vectors for the surface unit cell describe the triangular lattice of the substrate. They are related to the bulk basis by: $a_{surf}=[\bar{1}10]_{bulk}/2$, $b_{surf}=[0\bar{1}1]_{bulk}/2$ and $c_{surf}=[111]_{bulk}$. The h and k indexes are chosen to describe the in-plane momentum transfer [in reciprocal lattice units, (r.l.u.) of the NiO(111)] and ℓ the perpendicular momentum transfer. The chosen surface unit cell has a sixfold symmetry; due to the threefold symmetry of the bulk substrate an extra condition was imposed: the surface unit cell is such oriented to have a NiO Bragg peak at the (1,0,1) position in the reciprocal space. The reported integrated intensities were obtained through rocking scans and were corrected for monitor, background, polarization, and Lorentz factors.[20–24]

The x-ray beam was focused on the sample with a measured size of 350×450-μm full width at half maximum (vertical×horizontal). Adequate detector slits were chosen for all measurements yielding to an angular acceptance of the detector of 0.23°×0.23° for all the quantitative scans. More details concerning the used geometry and diffractometer can be found in Ref. 25. For all the in plane scans the incidence and exit angles were kept equal to $\alpha_c=0.17°$. This corresponds to $\ell=0$ inside the material and $\ell=0.05$ r.l.u. of NiO outside. The most meaningful regions in reciprocal space were systematically investigated: the in-plane $[h,h,0]$ and $[h,0,0]$ directions and the out-of plane crystal truncation rods [CTRs Refs. 26 and 27]. Since the GIXD chemical resolution is not able to distinguish between Ni, Fe, and Cu, high resolution (HR) and energy filtered (EF) transmission electron microscopy (TEM) measurements of cross sections were used to complete the structural characterization of the interfaces (using an electron microscope: Jeol 3010 LaB_6, working at 300-keV-energy). The detailed approach allowing drawing chemical maps is described in Ref. 28.

The magnetic hysteresis loops were measured using a vibrating sample magnetometer (VSM). The magneto-transport properties were obtained through giant magnetoresistance (GMR) measurements in a dc four in-line points (two voltage and two current contacts) current in plane (CIP) configuration (injected current i parallel to the surface plane). The external magnetic measurement field H_{ext}^{mes} was always in the surface plane and both longitudinal ($i \| H_{ext}^{mes}$) and transverse ($i \perp H_{ext}^{mes}$) measurements were performed. Indeed, these two measurements allow distinguishing the GMR effect from the classical magnetoresistance (MR) signal. For the GMR, the resistance of the sandwich increases in both cases (longitudinal and transverse) when passing through the antiparallel orientation of the magnetization of both layers, while for the MR, the signals measured in both cases are generally reversed and of lower amplitude, ~0.2%. Moreover, in the GMR, plateaus may appear, which is not the case in MR (the signal is peaked). For samples annealed in a saturating external field, H_{ext}^{sat}, the GMR measurements generally were performed such as ($H_{ext}^{mes} \| H_{ext}^{sat}$). In the situations where the magnetic in-plane anisotropy was investigated the sample was rotated in the direction-fixed H_{ext}^{mes} field. The sample magnetic history (if any) will be described from study to study in the next section.

III. RESULTS

Before growing thin films the surface morphology of the NiO(111) substrates after the preparation process described in Sec. II was checked by atomic force microscopy (AFM). Both air- and UHV- AFM were performed for samples having a mosaic spread less than 0.1°. The ultimate vertical resolution achieved in the contact mode UHV-AFM was about 3 Å; at that resolution, the surface exhibits flat micron sized terraces separated by steps of height of few nanometers.[16] The widths of the peaks observed by GIXD suggest diffracting domain sizes between 100 and 500 nm, depending on the sample preparation, indicating that the AFM-seen terraces might contain some structural defects (other than steps) which limit the coherence length to several hundreds of nm. As a matter of fact the NiO(111) single crystal surfaces we prepare are of high structural and morphological quality. The detailed preparation and characterization of our typical NiO(111) surfaces can be found in Refs. 15 and 16.

A smooth starting surface is mandatory for the growth of a complete spin valve since all layers must be continuous and smooth. In particular, it is well known that thickness inhomogeneities in the Cu non-magnetic layer, which may occur because of large defects on the starting surface, may magnetically couple both ferromagnetic layers (through pin holes) and prevent the onset of GMR. Much care has thus to be taken to determine the adequate growth conditions of the first (epitaxial) layer.

A. Growth of the ferromagnetic films on NiO(111)

1. Permalloy film on NiO(111)

We have investigated in detail the growth of the Py film at different growth temperatures. At room temperature the Py film has a very poor crystalline structure and is almost disordered. High resolution TEM images clearly show Py crys-

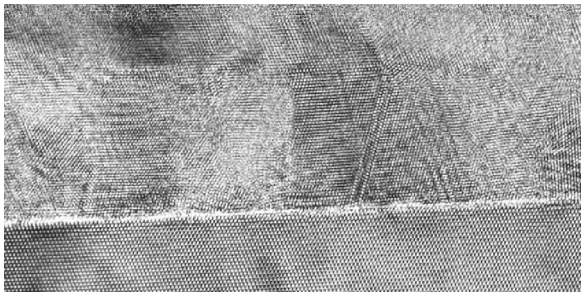

FIG. 1. Atomic resolution TEM image for a RT prepared Py/NiO(111) interface. The film (top) is polycrystalline and the interface is sharp and flat. The NiO(111) substrate (bottom) is of high quality.

tallites (Fig. 1). Interestingly, a similar behavior has been observed for the Co/NiO(111) interface prepared at RT.[29]

Direct growth or annealing (after RT growth) at very high temperatures (>800 K) leaves the Py film in a well crystallized state free from defects and stacking faults. At such temperatures the interface between Py and NiO(111) is fairly reactive and Fe deeply diffuses into the NiO substrate to form a spinel interface compound. The high oxidation/reduction reactivity of Fe/NiO interfaces has also been reported in Ref. 13. Bulk Ni-Fe-O spinels are ferrimagnetic and such a layer could prevent or modify the magnetic coupling, making more complex the understanding of the phenomena. Thus the high temperature preparation is not well suited for preparation of epitaxial spin valves within our approach. When the growth is performed at 600 K the spinel GIXD signal is always very small; the diffusion at the interface is thus limited to a very few atomic planes (as also checked by TEM).

The temperature of 600 K appeared to be suitable within the framework of obtaining an epitaxial spin valve. Figure 2 shows for such a sample a scan along a transfer momentum direction perpendicular to the surface ($[1.18,0,\ell]$), direction

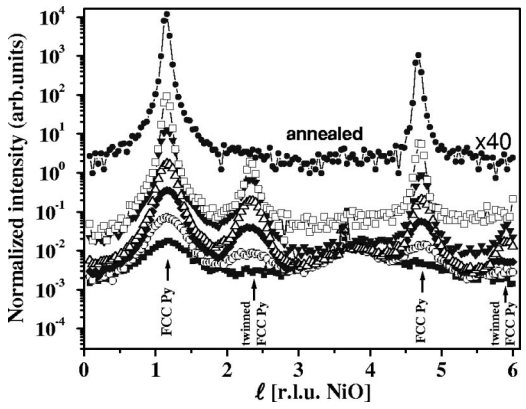

FIG. 2. Scan along a perpendicular direction to the surface (the $[1,0,\ell]_{Py}$ direction, i.e., the $[1.18,0,\ell]_{NiO}$), passing through Bragg peaks of the Py which are separated for the different stacking (fcc and twinned-fcc). From bottom to top, the Py thickness are: 3, 6, 12, 24, 50, 120, and 200 Å; the last situation is the annealed film and was vertically shifted ($\times 40$) for the sake of clarity. No more twinned fcc structure is present after the annealing.

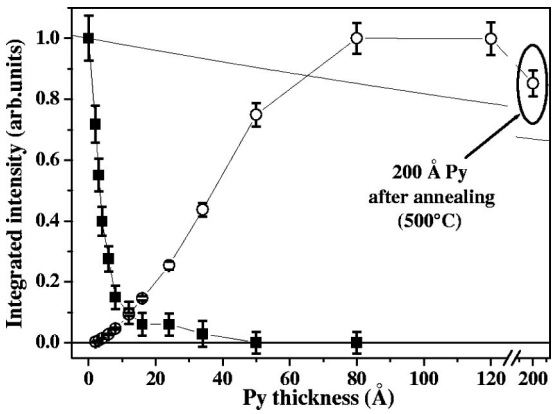

FIG. 3. Evolution of the scattered signal characteristic of the uncovered [still $p(2\times2)$ reconstructed] surface [the $(3/2,0,0)_{NiO}$ surface peak, filled symbols] and the ordered relaxed Py $(1,1,0)_{Py}$ (opened symbols), function of the deposited thickness of Py (please note the axis break). Both curves have been normalized. The continuous thin line shows the evolution of a $p(2\times2)$ signal due to the absorption in a continuous Py layer (absorption length in Py at 18 keV$=30.56$ μm, the curve was calculated for an incidence angle of 0.17°). The absorption in the Py layer cannot explain by itself the attenuation and vanishing of the NiO reconstruction signal.

passing through Bragg peaks which are well separated for the different stacking (the fcc and the twinned one of the Py). The structural quality is very good over large areas since GIXD probes areas of the sample of several square millimeters. The ratio of the integrated intensities of characteristic peaks of fcc and twinned-fcc Py structures (i.e., at $\ell=1.18$ and $\ell=2\times1.18$) shows that the film contains less than 5% of twinned FCC stacking. The increase in intensity of the peaks with respect to the amount of Py deposited shows that the whole film is single crystalline and epitaxial. The epitaxial relationships with respect to the substrate can be deduced from the position of in-plane Py peaks, along the $[h,h,0]$ and $[h,0,0]$ directions and are (111)Py//(111)NiO and [100]Py//[100]NiO.

While the Py deposition proceeds, the NiO $p(2\times2)$ reconstruction signal vanishes. Indeed, the divergence of the electrostatic potential is cancelled by the metallization as well as by the surface reconstruction, that becomes unnecessary when a metallic layer is deposited. The evolution of the signal of the NiO(111) surface reconstruction[15–17] thus allows one to monitor the coverage by the metallic layer. However, our data are hardly of any use to determine whether the reconstruction vanishes as a consequence of a movement of its atoms or simply by filling of the holes in the reconstruction with metal (Ni and Fe) atoms. The intensity recorded for the reconstruction signal is roughly proportional to the uncovered ratio of the surface. In Fig. 3 we show the evolution of the $(3/2,0,0)_{NiO}$ reconstruction peak with respect to the deposited thickness of Py(t_{Py}) as well as the evolution of the intensity at the $(1,1,0)_{Py}\equiv(1.18,1.18,0)_{NiO}$ Py position, its intensity being roughly proportional to the amount of deposited Py that adopts a fcc structure (twinned and not twinned). About 30–40 Å are necessary before the reconstruction signal vanishes indicating that the initial growth mode of Py is

a Volmer-Webber mode and is followed by coalescence. The detailed study of the growth mode with respect to the thickness and to the substrate temperature will be reported elsewhere.

Most of the samples described here were prepared at relatively high temperature (higher than the Néel temperature of the NiO, $T_N = 523$ K). If not otherwise specified, the samples were zero field (environment remanent field) cooled from their preparation temperature to RT. Even in these conditions, remarkably, for all growth temperatures the Py layer exhibits a very large coercivity that is at least an order of magnitude larger than usually expected for Py. Indeed, even the RT deposited polycrystalline Py layer exhibits a RT measured coercive field $H_c = 105 \pm 10$ Oe for a 170-Å thickness, without needing to onset the magnetic coupling by cooling from above T_N to RT in external magnetic field (procedure believed to magnetically couple the FM layer to the AF substrate by magnetic pinning). Comparatively, only 0.05 Oe is expected for a polycrystalline bulk sample and at most 10–20 Oe for an uncoupled single crystalline Py layer (see Sec. III B 1). The large increase of the coercivity of the Py layer deposited on single crystalline NiO(111) is due to the exchange coupling mechanism described before and suggests its use as magnetically hard (pinned) layer in a spin valve. The magnetic energy (obtained from the coercivity) at the interface is as large as $J_{Py/NiO}$(single crystal)$= 0.12$ mJ/m^2 and will be discussed in Sec. IV B. Although this approach may be somewhat crude it allows comparing quantitatively the exchange coupled interfaces. The present observations lead to the idea that preparing fully Py-based spin-valve devices on single crystalline NiO(111) substrates must be possible by exploiting the reproducible increase of coercivity that has almost not been reported in detail up to now, rather than the less easily controllable hysteresis loop shift. Moreover, the increase of the coercive field is not sample history dependent and appeared to be almost isotropic (variations with respect to the angle between H_{ext}^{sat} and H_{ext}^{mes} remain below 15%).

2. Co on NiO(111)

Using a similar GIXD approach we have previously shown[29] that the growth of Co on NiO(111) single crystals has some similarities with the growth of Py/NiO(111). For a substrate held at room temperature the growth is nearly polycrystalline and improves with increasing substrate temperature. Above 500 K the Co film is fully crystallized with many stacking faults. Increasing even more the substrate temperature during Co growth allows reaching perfect epitaxial fcc Co even for thick layers (>20 nm) without HCP or twinned fcc contributions. However, Co exhibits a strong Volmer-Weber growth mode (Fig. 4); even at 20-nm thickness large Co islands were observed by atomic force microscopy and the substrate is sometimes still visible. The three-dimensional growth of Co was further quantitatively investigated by small angle x-ray scattering experiments performed *in situ* in the 1–30-Å thickness range. A ≈ 0.7 sticking coefficient at 600 K was obtained and the actual diameter (respectively height) of the islands was ≈ 4 (respectively 2) times the incident Co thickness. Such a layer is thus not adequate at all for spin valves building.

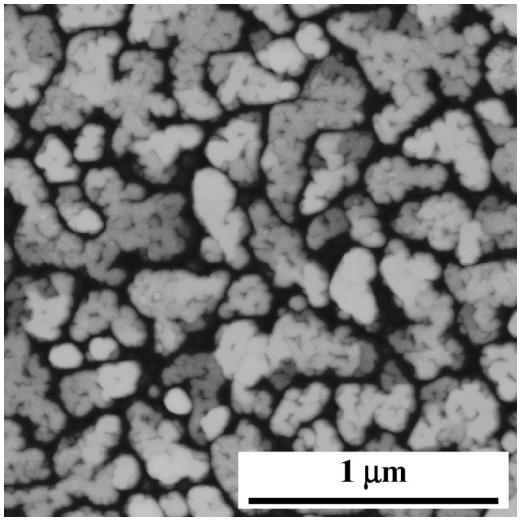

FIG. 4. AFM image of a 25-Å Au/200-Å Co/NiO(111) single crystal layer. The height color scale is 50 nm. The NiO substrate is still visible.

From the magnetism point of view we observed again huge coercivities of the Co layers.[29] For the Co/NiO(111) interfaces much attention was paid to the magnetic history of the samples. The investigated preparation methods included Co deposition under magnetic field at temperatures below and above T_N(NiO) as well as post-preparation annealing of the sample at 650 K, i.e., above T_N(NiO) and with a $H_{ext}^{sat} = 2.1$ kOe that was maintained during cooling to RT. Interestingly, the increase in coercivity was independent of the magnetic history of the sample. The well-crystallized samples show almost square hysteresis loops and Co acts as a harder (magnetically pinned) layer. The magnetic properties of samples prepared above 600 K have been investigated by VSM with respect to the measurement temperature. H_c increases with decreasing temperature and below 150 K (for samples annealed in the external magnetic field) the exchange field appears and has a similar behavior than H_c, with a maximum of 135 Oe at 50 K. These features undoubtedly confirm the onset of classical exchange coupling between the Co islands and the antiferromagnetic NiO(111) substrate at low temperatures. Measurements for different Co thicknesses (t_{Co}) in the 14–23 nm range for samples prepared at 800 K showed again a $H_c \propto t_{Co}^{-1}$ law and no hysteresis loop shift at room temperature.[29] Our interfacial magnetic energies (based on coercivity) $J = 1.27$ mJ/m^2 are again nearly an order of magnitude larger than those obtained for sputtered systems ($J = 0.11$ mJ/m^2 in Ref. 30).

3. $Co_{30}Fe_{70}$ on NiO(111)

Since epitaxial Ni on NiO(111) single crystals forms islands[17] and permalloy grows more layer wise, we tried to improve the Co growth by addition of Fe to obtain smoother and high coercive pinned layers. The growth of $Co_{30}Fe_{70}$ layers on NiO(111) single crystals was investigated by GIXD. Interestingly, $Co_{30}Fe_{70}$ adopts a body centered cubic

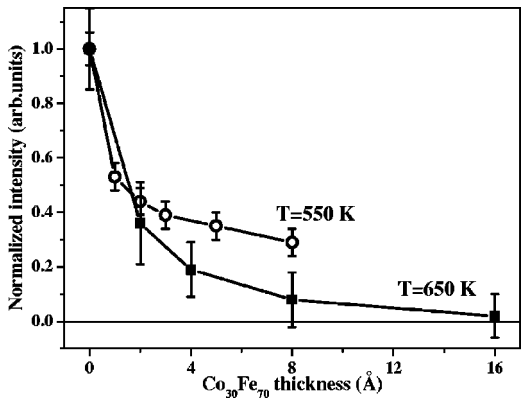

FIG. 5. Evolution of the $p(2\times2)$ NiO reconstruction signal vs. the thickness of the $Co_{30}Fe_{70}$ layer, for two deposition temperatures: 550 K and 650 K.

(bcc) crystalline structure which allows investigating the effect of the crystal structure on the growth and magnetic properties with respect to the growth temperature. Again the growth temperature strongly influences the crystalline quality of the obtained film: the higher the temperature, the better the crystalline quality and the smoother the film. Figure 5 shows that at 650 K thicknesses in the nanometer range are enough to completely remove the surface reconstruction signal indicating a continuous epitaxial layer.

For the growth at 650 K in plane and out of the surface plane GIXD scans show the presence of textured bcc ((110) epitaxy) and fcc ((111) epitaxy) crystalline structures. However, the bcc structure is of very poor quality (about 20° in-plane mosaicity) and preferentially align dense crystallographic directions parallel to the [100] direction of the NiO(111) surface. HR-TEM images show the presence of a polycrystalline continuous $Co_{30}Fe_{70}$ film formed by several grains (Fig. 6) and a diffuse interfacial layer (3-nm thickness). The overall crystalline quality of the $Co_{30}Fe_{70}$ alloy

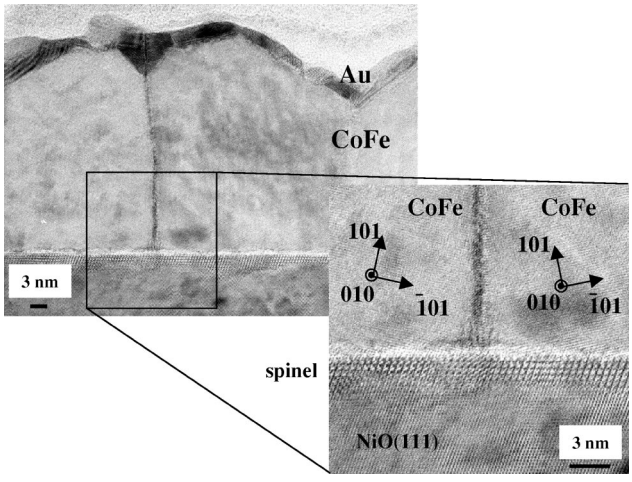

FIG. 6. Atomic resolution TEM image of the $Co_{30}Fe_{70}$/NiO(111) interface prepared at 650 K. The image shows the presence of a spinel layer at the CoFe/NiO interface position, due to Fe diffusion into the NiO substrate.

layer is thus very poor compared to Py and Co. The details of the growth studies will be reported elsewhere.

The coercivity of the $Co_{30}Fe_{70}$ film grown at 650 K and zero field cooled is increased to about 400 Oe for a 100-Å-thick film which makes possible its use as a pinned layer in spin valves. The interfacial energy amounts $J_{CoFe} = 0.64$ mJ/m^2 in this case. However, for films of very poor crystalline quality (grown at low temperature) and for diffuse interfaces (growth above 700 K) the magnetic coupling could not be observed and the interfacial energy reduces to 0.1 mJ/m^2 which is close to the value for a completely uncoupled film. We could thus effectively combine the wetting due to Fe with the high coercivity of the Co layer.

B. Spin valves

1. Py/NiO(111) based spin valves

The flatness of the different surfaces and interfaces in a spin-valve device is a known mandatory condition for obtaining a spin valve with usable GMR. For our first Py layer, this condition is fulfilled whatever the growth temperature is. We will now show that the control of the morphology of the first layer is not sufficient to obtain spin valves. For all studies reported in this section the initial NiO(111) single crystals were 5×5 mm^2 platelets of 0.5-mm thickness and had a 0.05° mosaic spread, $\approx$1500 Å domain size and $\approx$500 Å terrace size.

a. Room temperature prepared layers

A sample (#6 in Table I) for which all layers were deposited at RT on the substrate showed a classical MR of $\sim$0.2% and only one VSM hysteresis loop with a coercive field $H_c = 105\pm10$ Oe. The structure is not a spin valve since the FM layers are not decoupled by the Cu spacer.

In order to understand what mechanism prevents the onset of GMR, cross section TEM images were performed, showing a continuous rough metallic layer with the presence of well defined islands (Fig. 7, top left image). Only EF-TEM investigations allowed understanding the chemical morphology of the system (Fig. 7). From the chemical distribution maps (Cu, Ni, Fe) it appeared that although the Py layer in contact with NiO was quite flat, the deposited Cu forms islands on it. The sample is thus mainly made of a pinned 170-Å-thick Py layer with Cu inclusions. The observed coercive field is consistent with the total thickness of the Py and the $1/t_{Py}$ evolution of the coercivity that will be discussed in Secs. III B 1 d and IV B.

Additional HR-TEM cross section images showed that Cu grows mainly with a fcc (111) structure and preferentially on the (111) Py crystallites. This is consistent with the lower surface energy of Cu(111) compared to other orientations. Interestingly, the second Py layer seems to wet well the Cu surface whatever the morphology (Fig. 7). Thus, within our preparation conditions, getting a well defined epitaxial spin valve stacking reduces to make the first Py layer looking like a (111) single crystal surface. The control of only the morphology of the pinned Py layer was thus not a sufficient criterion in this system.

TABLE I. (Fully epitaxial) Py based spin valves using NiO(111) single crystalline substrates (#1–#6). The preparation conditions (SP indicates the standard preparation described at in II, (O^{2-}) an additional *in situ* O^{2-} etching of the substrate, A(970 K) an additional air annealing of NiO(111) at 970 K), the substrate temperature T during film growth and measured characteristics of the sandwiches and their different layers are given as well as RT measured coercivities of Py films deposited on NiO single crystals (#7–#10). The effective compositions were cross checked by chemical dosing.

	t_{pinned} Py (Å)	t_{spacer} Cu (Å)	t_{free} Py (Å)	H_c pinned Py (Oe)	H_c free Py (Oe)	GMR (%)	Remarks
#1	100	50	100	180	35	3.5	SP; (O^{2-}); $T=580$ K
#2	60	30	80	260	75	2.4-3.1	SP; $T=580$ K
#3	130	45	85	130	30	2.5-3.0	SP; $T=580$ K
#4	100	50	100	150	35	2.25	SP; (O^{2-})&A(970 K); $T=580$ K
#5	60	35	60	330	45	3-3.5	SP; (O^{2-})&A(970 K); $T=580$ K
#6	70	45	100	105	105	no GMR	SP; $T=$room temperature
#7	155	-	-	95	-	-	SP; $T=560$ K
#8	200	-	-	85	-	-	SP; $T=650$ K; film annealed at 800 K
#9[a]	308	-	-	44	-	-	SP; $T=650$ K
#10	115	-	-	105	-	-	SP; $T=600$ K

[a]The reported value for H_c (measured value, 180 Oe) is corrected with respect to the actual composition of $Ni_{96\pm3}Fe_{4\pm3}$ using Ref. 35.

b. First Py layer deposited at 600 K

A deposition temperature of 600 K for the first Py layer ensures a good crystallinity and an almost sharp interface. Moreover this temperature is above the NiO Néel temperature and the large Py magnetic susceptibility let expect a single magnetic domain structure for Py during the cool down to RT and in turn the occurrence of an exchange field H_E. A 25 Å Au/100 Å Py/50 Å Cu/100 Å Py/NiO(111) sample (#1 in Table I) was built on such a Py layer. All other layers were RT deposited. Prior to deposition the substrate was etched with O^{2-} ions for 20 minutes at 2keV (drain current $\sim 10\ \mu$A), this preparation will be discussed in more details in Sec. III B 1 d. The thicknesses were chosen to avoid GMR cancellation and must thus be understood as not optimized with respect to the GMR based sensors but realistic within the growth of a model epitaxial spin valve. Let us first discuss the magnetic properties.

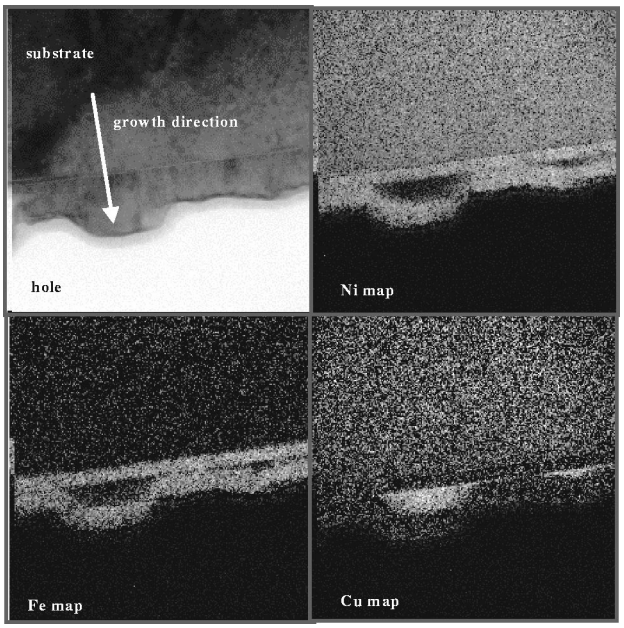

FIG. 7. EF-TEM images taken at the Ni, Fe and Cu $L_{2,3}$ edges of sample #6 in Table I. The two Py layers can be distinguished as well as the nucleation of the Cu cluster layer between them. The very thin continuous Cu film shows that the first Py layer is flat.

The VSM hysteresis loops were measured from 300 K down to 15 K (Fig. 8). Two individual loops can be fairly well distinguished even at RT [Fig. 8(a)] indicating almost no magnetic coupling between the Py layers i.e. almost no pin-holes in the Cu layer. As expected, the pinned Py layer acts as the hard magnetic layer and the top uncoupled Py layer as the soft sensing layer. Clearly, the center of gravity of the wider loop is shifted at 15 K with respect to the narrower loop (sensing layer, small H_c) due to the unidirectional exchange coupling with exchange field H_E which yields measurable values below 100 K [Fig. 8(b)]. Although no additional annealing under an external magnetic field was done the magnetic exchange coupling appears naturally in our samples more likely due to our preparation conditions (deposition above the NiO Néel temperature). The coercivity of the pinned layer increases with decreasing temperature, showing that all its magnetic properties are strongly affected by the NiO substrate [Fig. 8(b)], whereas the coercivity of the free Py layer remains constant ($\sim$40 Oe). Compared to sputtered Py films,[31,32] for which H_c values in the 1–10-Oe range were reported, the H_c values of our free Py layers are quite high. HR-TEM and EF-TEM images of such samples show defect free epitaxial layers and a sharp NiFe/NiO interface. It is thus reasonable to attribute the coercive field enhancement of the free Py layer to magneto-crystalline con-

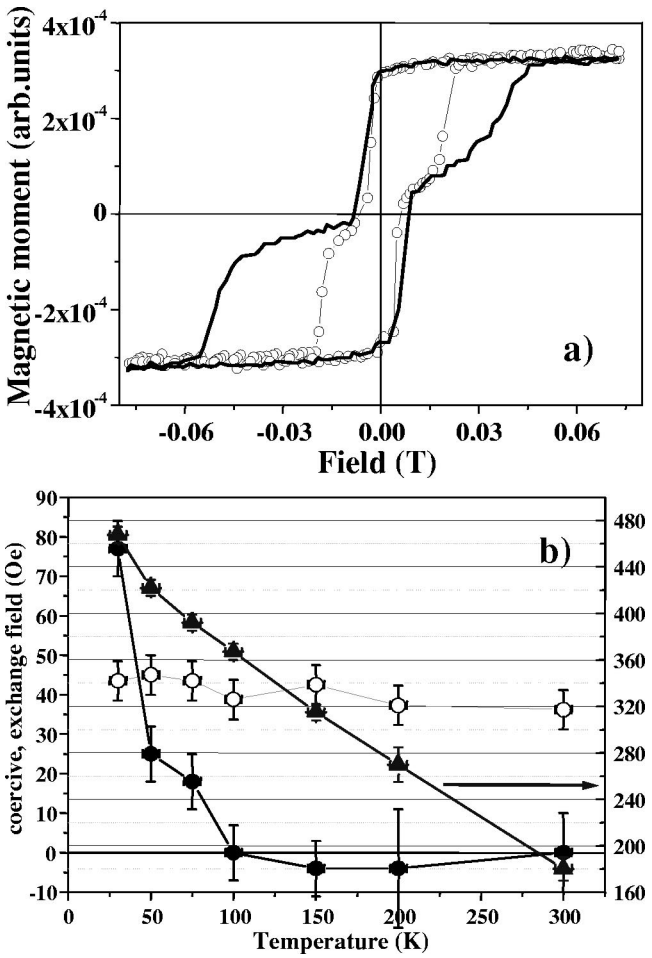

FIG. 8. (a) VSM hysteresis loops measured at 300 K (○) and 15 K (thick line) for a fully epitaxial 25 Å Au/100 Å Py/50 Å Cu/100 Å Py/NiO(111) spin valve. (b) H_E (●) and H_c (▲) of the pinned Py layer and H_c(○) of the free Py layer vs. temperature.

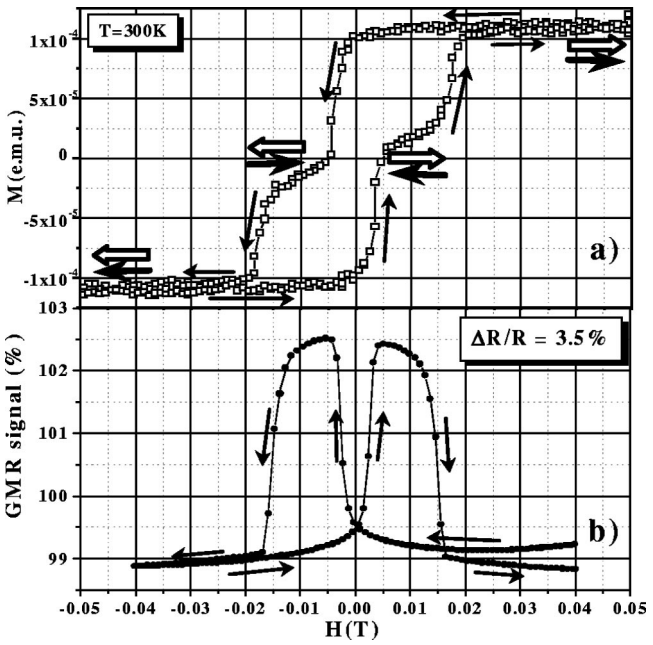

FIG. 9. Hysteresis loops measured by VSM (a) and GMR in CIP transverse geometry ($i \perp H_{ext}^{mes}$) (b) for the spin-valve described in Fig. 10 prior annealing showing a square GMR signal (maximal value of 3.5% and plateaus). On the top (VSM) curve the arrows show the relative orientation of the two magnetic layers: pinned layer (thick arrow) and free magnetic layer (open arrow). On both curves thin arrows are showing the path followed with the applied external field during the measurement.

tribution to the magnetic anisotropy although we cannot totally exclude an enhancement of the coercivity by an orange peel effect that could be induced by the particular morphology of the NiO(111) surface.

The different behaviors of the coercivity of both Py layers combined with the results from the RT grown sample unambiguously show that the free Py layer is neither pinned by the NiO substrate nor coupled to the pinned Py by pin-holes. The magnetoresistance measurements were performed at RT in the CIP geometry [Fig. 9(b)] for transverse and longitudinal GMR. The GMR equals to about 3.5% at the maximum and its variation along the top plateau is limited to 14% of the maximal value (i.e., 0.5% in the scale of Fig. 9b). The obtained device thus has all the magnetic features of an operational spin-valve sensor but is based on the pinned layer coercive field increase and not on the exchange field that is negligible in our samples at RT. In Fig. 9 the correspondence between the GMR and VSM measurements appears clearly. The characteristic magnetic properties of each film are very similar in both measurements, confirming again the absence of pin-holes. We shall conclude that the Cu spacer does a very good magnetic decoupling of both Py layers. Moreover the effect was stable during magnetic cycling at 50 Hz and the overall properties of our spin valve are almost sample history independent (as long as diffusion was prevented).

c. Thermal stability of the Py based spin valves

We have next used our model spin valves to tackle the important question of the thermal stability of the structure and of the magnetic properties. Annealing of exchange coupled layers at a temperature between the AF substrate Néel temperature (520 K for NiO) and the FM layer Curie temperature followed by a cooling to RT under a saturating magnetic external field is believed to generate or increase H_E because of the magnetic polarization of the FM layer.[33,34] A sample similar to the previous one has been annealed at 700 K for 10 minutes, then cooled down to RT under a magnetic field of 2.1 kOe. Surprisingly after this treatment both, the GMR response (2%) and the H_c value for the pinned layer, were found to decrease. TEM cross sections were used to understand the change of the magnetic properties (Fig. 10).

Remarkably, all the layers are epitaxial and on the atomic resolution TEM image [Fig. 10(a)] no defect can be found. The successive layers can be distinguished in the HR-TEM image and the interfaces between the different metallic layers remain all chemically sharp. To the contrary, the Py/NiO interface becomes wavy (because of the induced strain due to Fe diffusion) and diffuse: a spinel-like compound of ≈10-Å thickness, already observed by GIXD for high temperature growth and/or annealing, appears after the 700 K annealing of the complete spin valve. The EF-TEM measurements

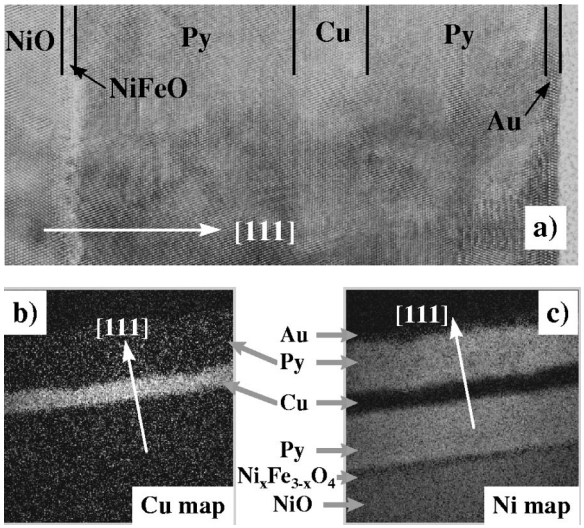

FIG. 10. (a) HR-TEM image with atomic resolution for a fully epitaxial 25 Å Au/100 Å Py/50 Å Cu/100 Å Py/NiO(111) spin valve after annealing at 700 K for 10 min. (b), and (c) EF-TEM chemical maps at the Cu $L_{2,3}$ and Ni $L_{2,3}$ edges. White contrast indicates the presence of the investigated element.

[chemical maps of all present elements, Figs. 10(b) and 10(c)] allowed quantifying the concentration profile across the interface showing a $Ni_xFe_{3-x}O_4$ compound with $1<x<2$. Details on the analysis of such diffuse interfaces can be found in Ref. 28. The formation of this compound degrades the properties of the spin valve. Several reasons may be invoked: (i) the ferrimagnetic interfacial spinel (since stoichiometric bulk trevorit ($NiFe_2O_4$) is known to be ferrimagnetic) may be less well magnetically coupled to NiO than Py; (ii) the interfacial compound may limit the volume of NiO that participates in the coupling; and (iii) the wavy interface may limit the efficiency of the specular reflectivity of electrons that may then lose their polarization after reflection. In any case, it appears that our spin valves are chemically stable up to 600 K but not above.

d. Sample preparation and effect of the Py thickness

In order to understand the influence of different parameters on the exchange coupling phenomenon and on the properties of epitaxial spin valves a set of samples was prepared (Table I) in different growth conditions. Different and well characterized initial substrate states were used. High temperature (1550 K) air annealed surfaces show a small Ca contamination and smooth surfaces; O^{2-} etching before deposition leads to rough and clean surfaces, a subsequent annealing at moderate temperature (970 K) in air, heals (partially) the surface roughness.[15–17] Whatever the substrate preparation method all samples show an increase of H_c with respect to the un-coupled film and nonzero H_E at low temperatures ($T<100$ K). A similar behavior has been observed for epitaxial Co islands deposited on single crystalline NiO(111) surfaces,[29] confirming that the present magnetic phenomena are related to the exchange coupling and not to the onset of interfacial compounds.

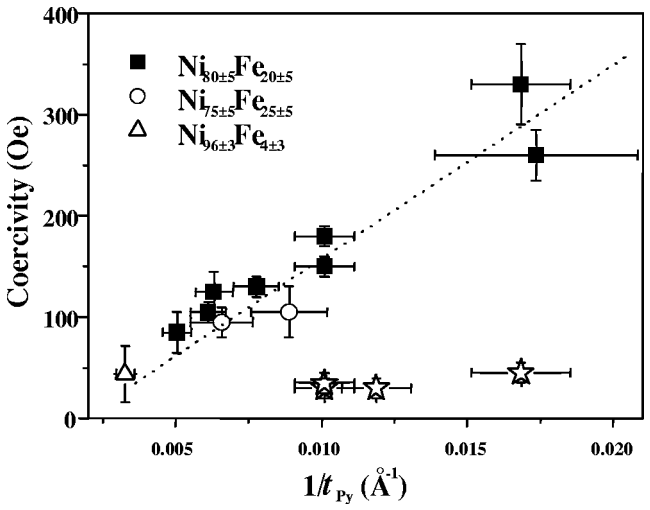

FIG. 11. The VSM measured coercivity H_c of the pinned Py layer is represented versus the inverse of its thickness, $1/t_{Py}$, for different compositions (checked by chemical etching). The coercivities were corrected with respect to the composition and corresponding magnetic permeability (Ref. 35). The dotted line is a linear fit $H_c = f(1/t_{Py}) = (15837.6 \pm 1899)$ Oe · Å $\times 1/t_{Py} + (4.3 \pm 16.6)$ Oe. Even if large error bars are present the offset (bulk coercivity) has the right order of magnitude (about 10 Oe). H_c for the free Py layer is also shown (opened stars). The typical error bars were estimated of about 10% for the thickness and 10-25 Oe for the coercivity.

The effect of the thickness of the pinned Py layers, t_{Py} was also investigated. Figure 11 shows the coercivity of the pinned Py layer for all samples of Table I: H_c is proportional to $1/t_{Py}$. Even for films as thick as 100 Å of Py the coercivity is enhanced to values of several hundreds of Oe that typically correspond to the values reported for Co based sputtered spin valves.[30,36,37] And indeed, the interfacial energy $J(J=M_s t_{Py} H_c$, where M_s is the spontaneous magnetization of bulk Py: 800 mJ/m^2) is of the same order of magnitude as for sputtered Co/NiO interfaces[30] [$J_{Py/NiO}$(single crystal)$=0.12$ mJ/m^2 vs $J_{Co/NiO}$(sputtered)$=0.11$ mJ/m^2]. Hence, from a magnetic point of view a single crystalline Py/NiO interface is worth a sputtered Co/NiO(111) one and thus, *our Py layers can be used as pinned hard magnetic layers in fully epitaxial spin valves.*

Due to the smaller Cu thickness used for sample #2, both Py layers are not completely magnetically decoupled: H_c of the free Py layer is 75 Oe which is about twice larger than the value obtained for the other systems. The GMR signal is identical to the one of sample #3 showing that the gain in GMR due to thinner layers (pinned, free and spacer[9,30,38–40]) (compare #4 and #5 for example) is lost by the presence of pin holes in the spacer layer. Thus for our Py based spin valves the minimal Cu spacer thickness has to be 30–35 Å. Except the initial roughness, samples #1 and #4 are identical. Interestingly, a rough NiO substrate (#1) leads to better defined structures and magnetic properties i.e. a squarer GMR response signal (Fig. 12). The coercive field strengths are alike but the GMR signal is significantly larger. It is likely that the roughening of the NiO surface following the oxygen etching increases the nucleation density of the Py on

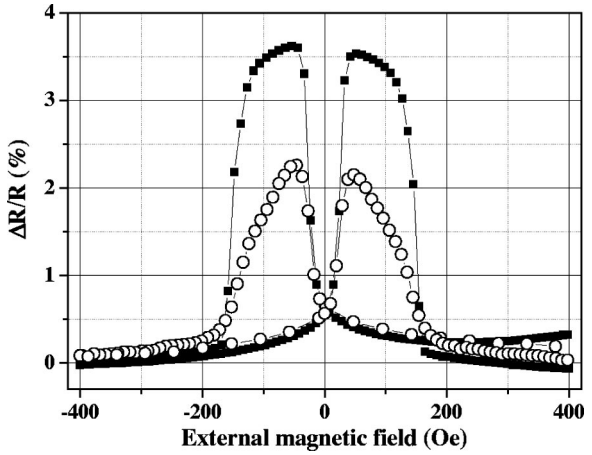

FIG. 12. GMR loops in transverse CIP geometry ($i \perp H_{ext}^{mes}$) measured for samples using a rough NiO surface (#1 square response with plateaus: filled squares) and a clean and flat NiO substrate (#4 peaked response: open circles).

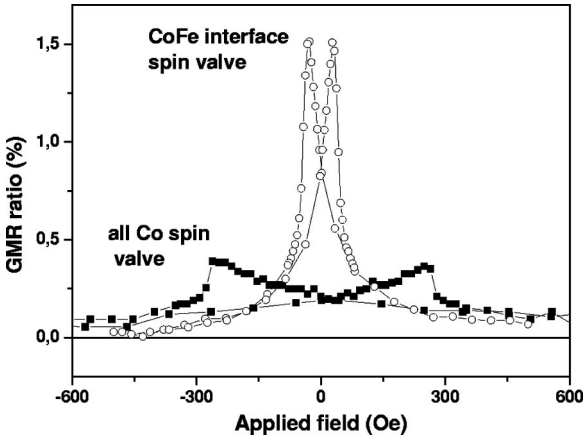

FIG. 13. GMR signal measured in transverse geometry for the all-Co and $Co_{30}Fe_{70}$ wetting layer epitaxial spin valves.

the surface, leading thus to a flatter Py film. This might then, in turn, influence the efficiency of the Cu layer as spacer through an improved wetting (compare samples #2 and #5). For the GMR response too, a higher nucleation density for magnetic domains during the magnetization reversal allows understanding the beneficial contribution from substrate roughening. In summary, our preparation methods can yield, in a reproducible manner, GMR values around 3% for spin valves fully based on Py. The best substrate is a rough O^{2-} etched NiO(111) single crystal surface. A large thickness (50–130 Å) for the pinned layer (to get a continuous film) and Cu films thicker than 35 Å (Fig. 10) are required, limiting thus the maximal GMR values. The exchange coupling exhibits two features: (i) below 100 K a unidirection exchange field H_E that increases with decreasing temperature, and (ii) a strong and almost in-plane isotropic enhancement of the coercive field $H_c \propto 1/t_{Py}$ at RT. The RT functioning of our spin valves is based on the increase in the value of H_c for the pinned FM.

2. Co/NiO(111) based spin-valves

The characteristics of the most interesting Co/NiO(111) spin valves are reported in Table II. Because of the strongly 3D (islands) growth mode of Co on NiO(111), attempts to produce spin valves with 100 and 200 Å of Co as pinned layer failed. Only using 300-Å Co (sample #11) a GMR response could be obtained and it is as small as 0.4%.

Most of the $Co_{30}Fe_{70}$ based spin valves do not show GMR signal. The reason is mainly the morphology of the pinned layer. The formation of individual large bcc alloy grains (Fig. 6) leads, albeit the good surface wetting, to a very rough layer. The GMR remains generally essentially zero. Even if some GMR might exist (as for sample #13), pinholes may be present since the H_c of the free layer is large. Moreover for the $Co_{30}Fe_{70}$ layer the surface preparation plays a major role, an O^{2-} etching (sample #14) improves drastically the magnetic coupling (compare to sample #13) because of a better initial wetting but the GMR degrades mainly because the roughness of the $Co_{30}Fe_{70}$ layer increases. Obviously, the morphology and the poor crystalline quality of the $Co_{30}Fe_{70}$ layer make it a poor candidate as pinned magnetic layer with our preparation methods. The quality of the magnetic coupling appeared to be much more sensitive to surface preparation than for Co or Py.

The improved wetting of the NiO substrate due to the presence of Fe is an interesting property that we have tried to use in Co/NiO(111) based spin valves. We have prepared an epitaxial spin valve using Co as pinned layer with a 8-Å-thick $Co_{30}Fe_{70}$ wetting layer on a NiO(111) single crystal (sample #12). The preparation conditions were kept identical with respect to sample #11 except the incorporation of 0.1% Cu in the top Co layer in order to render it magnetically softer. The result is remarkable (Fig. 13), the GMR increases from 0.4% to 1.5% although the coercivity of the pinned layer is reduced by about 25% because of the presence of the interfacial alloy. Thus a thin $Co_{30}Fe_{70}$ layer is an

TABLE II. Co and $Co_{30}Fe_{70}$ based spin valves using NiO(111) single crystalline substrates.

	t_{pinned} (Å)	t_{spacer} Cu (Å)	t_{free} (Å)	H_c pinned (Oe)	H_c free (Oe)	GMR (%)	Remarks (see Table I)
#11	Co(300)	50	Co(300)	370	330	0.4	SP; (O^{2-}); $T=650$ K
#12	$Co_{30}Fe_{70}$(8)+Co(292)	50	(Co+0.1% Cu)(300)	270	60	1.5	SP; (O^{2-}); $T=650$ K
#13	$Co_{30}Fe_{70}$(100)	50	Py(100)	140	70	0.5	SP; $T=680$ K
#14	$Co_{30}Fe_{70}$(100)	50	Py(100)	450	40	0.2	SP; (O^{2-}); $T=680$ K

excellent wetting layer that is able to improve the overall properties of the spin valves.

IV. DISCUSSION

A. Wetting effect of Fe

When Co and Ni are deposited on NiO(111), they exhibit a strong three-dimensional (3D) growth mode, with formation of metallic islands on the surface (as shown in Fig. 4). The addition of Fe to these metals allows a very good wetting of the surface and the growth appeared to improve a lot as far as wetting is considered. From another point of view, growing the alloys above 600 K leads to a diffuse interface which is detrimental to the H_c and GMR effect. The chemical composition of the diffuse layer is $Fe_{3-x}Ni_xO_4$.[28] Since the enthalpy of formation of NiO [$\Delta G(\mathrm{NiO}) = -13.36$ UA] is larger than that of Fe_3O_4 [$\Delta G(Fe_3O_4) = -19.02$ UA] it seems clear that the improved wetting is due to the thermodynamically favorable formation of the Fe oxide rather than to any more subtle surfactant or surface energy effect. However the final effect is a better growth of the alloys and may be transposed to sputtered spin valves.

B. Exchange coupling for single crystalline FM/NiO(111) interfaces

Our present studies of epitaxial spin valves allow one to draw some interesting conclusions about the exchange coupling mechanism itself. For all our films that are exchange coupled we observe a very large and reproducible increase of the coercivity, which can neither be completely attributed to the single crystalline structure of the layers nor to some interface compound nor to dead magnetic layers.[41] The additional magnetic energy is thus essentially due to the coupling mechanism and justifies the use of H_c in the evaluation of the magnetic interfacial energy *J*, at least in order to compare our interfaces.

Whereas the exchange field in FM/AF interfaces has been investigated thoroughly over decades the H_c increase due to exchange coupling has attracted attention only recently although sputtered samples have also shown, even modestly, this effect.[31,32,42] The model of Zhang *et al.*[43] suggests a $H_c \propto t_{FM}^{-3/2}$ law at low temperature derived from the statistically fluctuating energy of the pinned FM domain walls in an external magnetic field. Since we investigated the H_c behavior with respect to t_{FM} at room temperature it seems not surprising that this model does not account well for our results. The $H_c \propto t_{FM}^{-1}$ behavior has been foreseen in a model proposed recently by Stiles and McMichael.[44] These authors considered polycrystalline FM/AF interfaces and evaluated the H_c increase due to the FM layer because of inhomogeneous coupling to the AF and energy losses in the AF due to irreversible transitions of the antiferromagnetic order in the AF grains. The first phenomenon leads to a $H_c \propto t_{FM}^{-2}$ law at law temperatures that requires a contribution from intergranular exchange coupling in the ferromagnetic film. Since our Co films are made of single crystalline islands, our Py films are almost defect free and the measurement temperature we used (RT) was already relatively high, this first effect cannot contribute to the H_c increase here. The second phenomenon yields the $H_c \propto t_{FM}^{-1}$ behavior that we obtained experimentally on Co and Py films deposited on single crystalline NiO(111).

In the light of this model[44] we may quantify our results. Since the Py films have well defined thicknesses (2D growth) we focus on them. From the $H_c \propto t_{Py}^{-1}$ law we can extract a NiO domain-wall energy σ of 0.22 $\mathrm{mJ/m^2}$ at RT. Its value is of the expected order of magnitude for the weak six-fold anisotropy of the easy (111) plane. This value is about 3 times larger than previous measurements[45,46] but it has already been recognized that this energy increases with increasing NiO crystal quality.[46] Since our samples proved to be of single *T* domain with multiple *S* domains[41] and have very small mosaic spreads, our value may be closer to the NiO intrinsic domain-wall energy of the easy (111) plane. Importantly, our σ value indicates that rotation of the spins outsides the (111) plane can be excluded (as long as the magnetic field is applied in the sample plane) and thus contributions from the more anisotropic directions to the exchange coupling phenomenon. Note that within this mechanism the AF domain wall deeply (~ 2 μm, Ref. 45) extends in the NiO crystal. An intermediate situation was obtained for Py films deposited on single crystalline NiO(001) (Ref. 11) were the observed domain-wall energy includes contributions from the magnetic hard axis and in turn larger H_E values and an interface energy (0.08 $\mathrm{mJ/m^2}$) that lies in between our results (0.12 $\mathrm{mJ/m^2}$) and the value for sputtered NiO layers (0.03 $\mathrm{mJ/m^2}$). The observation of large interfacial energies is another confirmation that the model given in Ref. 44 applies well to our single crystalline interfaces.

From the onset temperature of H_E, knowing σ, we extract a FM/AF domain area of $\sim(530)^2$ $\mathrm{Å}^2$ which matches the typical terrace size (measured by AFM) of the NiO(111) single crystal substrates confirming that interface defects break the in-plane exchange coupling and not only grain boundaries. Across any of these defects the magnetization directions of the AF spins are uncorrelated, which is the main assumption in the model of Stiles and McMichael.[44] Our observations indicate that during cycling the external magnetic field, because of the large interface energies, the magnetization of the FM layer drags the magnetization of large AF volumes, as a consequence of the deep extension of the domain-wall inside NiO. The result is the observed increased H_c values because of the energy losses in the AF due to irreversible transitions of the AF order in the grains. We can now draw a more general picture of the magnetic exchange coupling at FM/AF interfaces. The phenomenon obviously has two competing feature:

(1) A net interfacial magnetization leading to the exchange field H_E; the AF has a finite magnetic domain size structure and in each domain the FM layer receives a statistically net field inducing the exchange bias by the random interaction first proposed by Malozemoff.[47,48] Large H_E values require large AF domain-wall energies and thus large in-plane magnetic anisotropies but the actual H_E value strongly depends on the magnetic history of the sample.

(2) An increased coercive field H_c for the pinned FM layer because of the energy losses in the AF when the magnetization of the AF is dragged by the FM one. This effect is

not dependent on the magnetic history of the sample and is enhanced when the interfacial energy is large, the AF domain-wall energy is small (leading to deep domain-walls) and the defect free in-plane FM/AF contact area size is large.

The studies reported here almost ideally illustrate the second case. Smaller grain sizes in the FM layer can only reduce the coercive field increase because of the $H_c \propto t^{-2}$ (Ref. 44) or $H_c \propto t^{-3/2}$ (Ref. 43) contributions arising from the magnetic interaction between FM grains. Smaller grain sizes in the AF should contribute to a limitation of this effect too, but may also lead to additional in-plane anisotropies and in turn larger H_E values. This point is confirmed by the results of Michel,[12] who reported a larger H_E for a polycrystalline film (66 Oe) compared to an epitaxial one (36 Oe) that had a larger coercivity. For Py on single crystalline CoO(111) an H_E (respectively H_c) increase (respectively decrease) with respect to decreasing interface quality was also observed.[10] Interestingly, single crystalline interfaces build on surfaces with the NiO (111) planes perpendicular to the interface should cancel the H_c increase but since the pure AF spin planes will then be perpendicular to the FM layer H_E may be cancelled too. A single crystalline AF substrate with pure spin planes parallel to the surface having a large in-plane unidirectional magnetic anisotropy should correspond to the almost ideal first case. All other situations should than have properties in between both ideal cases. Assessing this last assumption requires further experimental work.

The large H_c is now understood as part of the exchange coupling and is related to the good crystalline quality of both the epitaxial film and the substrate. It has the major advantage to be independent of the magnetic history of the sample and is the basic phenomenon used in our spin-valves.

C. Spin valves

Since sputtered Py layers only exhibit a modest increase of the coercivity and almost no shift of the hysteresis loop, it is not possible to directly compare our spin valves with similar ones made by sputtering. However, our results compare well with the typical properties of Co based spin valves.[30] Their typical structure is 100-Å Co or Py/35-Å Cu/(16-34) Å Co/300 Å NiO/Si. They have square response, maximal GMR about 10% and coercive fields in the 100-400 Oe range (depending on the Co thickness) and about 5 Oe for the pinned Co and free Py layer respectively.

Considering the thick layers we deposited, our 3.5% GMR is a rather big value. A simple calculation[49] shows that with optimized thickness (40–50-Å pinned layer and 25–30-Å Cu spacer) a 15–20 % GMR response might be achieved. Unfortunately it means also that the NiO surface should be flat over square millimeters. This target seems not obvious at all with single crystals and would need further improvements in surface quality. Keeping in mind that our structures are model spin valves, it is only important that they exhibit the right GMR effect in order to understand the role of each interface. Their optimization in terms of GMR response was thus not a goal in the present studies.

The very large thickness of the used Py layers makes this system not suitable for an application (reading device) due to the large shunting in the metallic layer. However, here we have a model system for which the influence of different parameters can be controlled and studied.

We have shown that the overall magnetic properties of our Py/NiO spin valves may be compared with sputtered Co/NiO based spin valves.[30] Several major differences may be highlighted: (i) we use Py as soft and hard magnetic layer; (ii) the complete structure is fully epitaxial; (iii) we use much larger Cu layer thickness limiting thus the problems due to pin-hole formation; and (iv) in the present case the resulting GMR is isotropic and *no annealing under a magnetic field is necessary to produce a functioning device*. Within a production process these features might be less stringent than the usual devices, except for the use of single crystalline substrates.

The achieved GMR is quite large, considering the nonoptimized thickness. Moreover, sizes for GMR sensors prepared by sputtering for industrial applications are typically of several square microns[2,3,50]; in the case of the epitaxial spin valves on NiO(111) single crystals substrates (5×5 mm^2 size of the sample), we ensured a good homogeneity and quality of the layers on a mm length-scale (distance between points in GMR measurements). It is very likely that the presence of defects at large length scale (μm terraces and nm steps on AFM images) decrease the macroscopically measured GMR signal. The reported values must thus be understood as lower limit.

V. CONCLUSION

We have shown that fully epitaxial spin valves with the desired magnetoresistive properties can be prepared and that they have at least similar properties to sputtered devices. The preparation conditions are reported in detail. The best results were obtained using Py as a magnetically pinned layer. We have shown that for molecular beam epitary prepared sandwiches, the flatness and the crystallographic structure of the pinned Py layer have to be controlled to reach an operational device. Even if the first layer is quite flat, a poor crystallographic quality leads to preferential nucleation of spacer clusters instead of a continuous layer preventing the decoupling of the magnetic layers. The best results are obtained within a compromise between the crystalline structure (growth temperature just below the onset of diffusion, 600 K) and the surface roughness (the GMR signal is better for oxygen etched surfaces) leading to single-crystalline epitaxial layers and good magnetic properties.

When NiO(111) single crystalline substrates are used, an increase of an order of magnitude of the coercivity of ferromagnetic layers in contact with the substrate is obtained. This effect is intrinsically part of the exchange coupling and is linked to the cooperative rotation (because of the large interfacial energy) of the ferromagnetic and antiferromagnetic domains during magnetization reversal. We have shown, by comparison with recent models, that the coercive field increase is driven by the irreversible transitions in the AF domain structure of NiO. The interfacial energy for single crystalline Py layers on NiO(111) equals that of Co/NiO interfaces prepared by sputtering enabling the use of Py as hard and soft magnetic layers when the substrate is a

single crystal. The corresponding effect for sputtered Py/NiO interfaces (if any) is much smaller.

For these spin valves the respective role of each interface can be investigated in detail. In particular, our model spin-valves that are fully characterized enabled us to highlight some important points: (i) the detrimental effect of interfacial diffusion of Fe into NiO on the GMR amplitude; (ii) the minimal Cu thickness of 35 Å, necessary to decouple the ferromagnetic layers; (iii) the increase of the GMR for etched surfaces; (iv) the very large exchange coupling energies; (v) the negligible role of sub monolayer Ca contamination; and (vi) the very important role of the coercivity increase which is completely linked to the crystalline quality in the exchange coupling phenomenon.

ACKNOWLEDGMENTS

B. Dieny is acknowledged for fruitful discussions, S. Auffret for support during the magnetic measurements, Y. Samson for the AFM measurements, G. Renaud for help during the early GIXD experiments, and M. Noblet for technical assistance during the growth of the spin-valve samples.

*Now at Max Planck Institut für Metallforschung, Heisenbergstr.1, D-70569 Stuttgart, Germany. Electronic address: cmocuta@mf.mpg.de

†Corresponding author. Electronic address: abarbier@cea.fr

[1] J. C. S. Kools, IEEE Trans. Magn. **32**, 3165 (1996).

[2] Y. Hamakawa, H. Hoshiya, T. Kawabe, Y. Suzuki, R. Arai, K. Nakamoto, M. Fuyama, and K. Sugita, IEEE Trans. Magn. **32**, 149 (1996).

[3] K. Nakamoto, Y. Kawato, Y. Suzuki, T. Hamakawa, T. Kawabe, K. Fujimoto, M. Fuyama, and Y. Sugita, IEEE Trans. Magn. **32**, 3347 (1996).

[4] W. L. Roth, J. Appl. Phys. **31**, 2000 (1960).

[5] J. Baruchel, M. Schlenker, K. Kurosawa, and S. Saito, Philos. Mag. **43**, 835 (1981).

[6] W. F. Egelhoff, Jr., T. Ha, R. D. K. Misra, Y. Kadmon, J. Nir, C. J. Powel, M. D. Stiles, R. D. McMichael, C. L. Lin, J. M. Sivertsen, J. H. Judy, K. Takano, A. E. Berkowitz, T. C. Anthony, and J. A. Brug, J. Appl. Phys. **78**, 273 (1995).

[7] W. F. Egelhoff, P. J. Chen, C. J. Powell, M. D. Stiles, R. D. McMichael, J. H. Judy, K. Takano, and A. E. Berkowitz, J. Appl. Phys. **82**, 6142 (1997).

[8] H. J. M. Swatgen, G. J. Strijkers, P. J. H. Bloemen, M. M. H. Willekens, and V. J. M. De Jonge, Phys. Rev. B **53**, 9108 (1996).

[9] S. Araki, M. Sano, Y. Tsuchiya, O. Redon, T. Saski, N. Ito, K. Terunuma, H. Morita, and M. Matsuzuki, J. Appl. Phys. **87**, 5377 (2000).

[10] T. J. Moran, J. M. Gallego, and I. K. Shuller, J. Appl. Phys. **78**, 1887 (1995).

[11] S. M. Rezende, M. A. Lucena, A. Azevedo, A. B. Oliveira, F. M. de Aguiar, and W. F. Egelhoff, Jr., J. Magn. Magn. Mater. **226–230**, 1683 (2001).

[12] R. P. Michel, A. Chaiken, C. T. Wang, and L. E. Johnson, Phys. Rev. B **58**, 8566 (1998).

[13] T. J. Regan, H. Ohldag, C. Stamm, F. Nolting, J. Luening, and J. Stoehr, Phys. Rev. B **64**, 214422 (2001).

[14] J. Nogués, T. J. Moran, D. Lederman, I. K. Schuller, and R. V. Rao, Phys. Rev. B **59**, 6984 (1999).

[15] A. Barbier, C. Mocuta, H. Kuhlenbeck, K. F. Peters, B. Richter, and G. Renaud, Phys. Rev. Lett. **84**, 2897 (2000).

[16] A. Barbier, C. Mocuta, and G. Renaud, Phys. Rev. B **62**, 16 056 (2000).

[17] A. Barbier and G. Renaud, Surf. Sci. Lett. **392**, L15 (1997).

[18] D. Wolf, Phys. Rev. Lett. **68**, 3315 (1992).

[19] ESRF Web site, http://www.esrf.fr.

[20] C. Schamper, H. L. Meyerheim, and W. Moritz, J. Appl. Phys. **26**, 687 (1993).

[21] M. F. Toney and D. G. Wiesler, Acta Crystallogr. Sect. A: Found Crystallogr. **49**, 624 (1993).

[22] E. Vlieg, J. Appl. Crystallogr. **30**, 532 (1997).

[23] E. Vlieg, J. Appl. Crystallogr. **31**, 198 (1998).

[24] O. Robach, Y. Garreau, K. Aid, and M. B. Véron-Jolliot, J. Appl. Crystallogr. **33**, 1006 (2000).

[25] R. Baudoing-Savois, G. Renaud, M. De Santis, A. Barbier, O. Robach, P. Taunier, P. Jeantet, O. Ulrich, J. P. Roux, M. C. Saint-Lager, A. Barski, O. Geaymond, G. Bérard, P. Dolle, M. Noblet, and A. Mougin, Nucl. Instrum. Methods Phys. Res. B **149**, 213 (1999).

[26] I. K. Robinson, Phys. Rev. B **33**, 3830 (1986).

[27] S. R. Andrews and R. A. Cowley, J. Phys. C **18**, 6427 (1985).

[28] P. Bayle-Guillemaud, A. Barbier, and C. Mocuta, Ultramicroscopy **88**, 99 (2001).

[29] C. Mocuta, A. Barbier, G. Renaud, and B. Dieny, Thin Solid Films **336**, 160 (1998).

[30] C. Cowache, B. Dieny, S. Auffret, M. Cartier, R. H. Taylor, R. O'Barr, and S. Y. Yamamoto, IEEE Trans. Magn. **34**, 843 (1998).

[31] V. I. Nikitenko, V. S. Gornakov, L. M. Dedukh, Y. P. Kabanov, A. F. Khapikov, A. J. Shapiro, R. D. Shull, A. Chaiken, and R. P. Michel, Phys. Rev. B **57**, R8111 (1998).

[32] V. I. Nikitenko, V. S. Gornakov, L. M. Dedukh, Y. P. Kabanov, A. F. Khapikov, A. J. Shapiro, R. D. Shull, A. Chaiken, and R. P. Michel, J. Appl. Phys. **83**, 6828 (1998).

[33] W. H. Meiklejohn and C. P. Bean, Phys. Rev. **102**, 1413 (1956).

[34] W. H. Meiklejohn and C. P. Bean, Phys. Rev. **105**, 904 (1957).

[35] *Condensed Matter Handbook*, edited by K.H. Nellwege and O. Madelung, Landolt-Börnstein, New Series, Group. III, Vol. 19a (Springer-Verlag, Berlin, 1986).

[36] H. D. Chopra, B. J. Hockey, J. P. Chen, R. D. McMichael, and W. F. Egelhoff, Jr., J. Appl. Phys. **81**, 4017 (1997).

[37] S. F. Cheng, J. P. Teter, P. Lubitz, M. M. Miller, L. Hoines, J. J. Krebs, D. M. Schaefer, and G. A. Prinz, J. Appl. Phys. **79**, 6234 (1996).

[38] R.-Y. Fang, T.-Y. Chen, Y.-L. Yu, and D.-S. Dai, J. Appl. Phys. **82**, 3957 (1997).

[39] C. Tsang, N. Heiman, and K. Lee, J. Appl. Phys. **52**, 2471 (1981).

[40] B. Dieny, V. S. Speriosu, S. Metin, S. S. P. Parkin, B. A. Gurney, P. Baumgart, and D. R. Wilhoit, J. Appl. Phys. **69**, 4774 (1991).

[41] W. Neubeck, C. Vettier, F. de Bergevin, F. Yakhou, D. Mannix, O. Bengone, M. Alouani, and A. Barbier, Phys. Rev. B **63**, 134430 (2001).

[42] V. I. Nikitenko, V. S. Gornakov, L. M. Dedukh, A. J. Shapiro, R.

D. Shull, and A. Chaiken, in *Proceedings of Spring'98 Materials Research Society Meeting*.
[43] S. Zhang, D. V. Dimitrov, G. C. Hadjipanayisb, J. W. Cai, and C.L. Chien, J. Magn. Magn. Mater. **198–199**, 468 (1999).
[44] M. D. Stiles and R. D. Michael, Phys. Rev. B **63**, 064405 (2001).
[45] M. D. Stiles and R. D. Michael, Phys. Rev. B **59**, 3722 (1999).
[46] K. Kurosawa, M. Miura, and S. Saito, J. Phys. C **13**, 1521 (1980).
[47] A. P. Malozemoff, Phys. Rev. B **35**, 3679 (1987).
[48] A. P. Malozemoff, J. Appl. Phys. **63**, 3874 (1988).
[49] B. Dieny, J. Phys.: Condens. Matter **4**, 8009 (1992).
[50] C. H. Tsang, R. E. Fontana, Jr., T. Lin, D. E. Heim, B. A. Gurney, and M. L. Williams, IBM J. Res. Dev. **42**, 103 (1998).